Thermal Loading and Lifetime Estimation for Power Device Considering Mission Profiles in Wind Power Converter

Ke Ma, *Member, IEEE*, Marco Liserre, *Fellow, IEEE*, Frede Blaabjerg, *Fellow, IEEE*, and Tamas Kerekes, *Member, IEEE*

***Abstract*—As a key component in the wind turbine system, the power electronic converter and its power semiconductors suffer from complicated power loadings related to environment, and are proven to have high failure rates. Therefore, correct lifetime estimation of wind power converter is crucial for the reliability improvement and also for cost reduction of wind power technology. Unfortunately, the existing lifetime estimation methods for the power electronic converter are not yet suitable in the wind power application, because the comprehensive mission profiles are not well specified and included. Consequently, a relative more advanced approach is proposed in this paper, which is based on the loading and strength analysis of devices and takes into account different time constants of the thermal behaviors in power converter. With the established methods for loading and lifetime estimation for power devices, more detailed information of the lifetime-related performance in wind power converter can be obtained. Some experimental results are also included to validate the thermal behavior of power device under different mission profiles.**

***Index Terms*—IGBT, lifetime prediction, mission profiles, power semiconductor device, thermal cycling, wind power.**

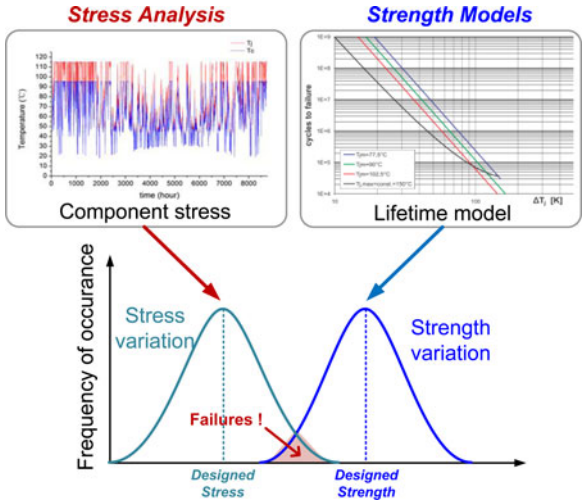

Fig. 1. Physics-based lifetime estimation for power electronic components.

I. Introduction

THE fast growth in the total installation and individual capacity makes the failures of wind turbines more critical for the power system stability and also more costly to repair [1]–[3]. Former field feedbacks have shown that the power electronics tend to have higher failure rate than the other parts in the wind turbine system [4], [5]. As a result, correctly estimating the reliability performance of the wind power converter is crucial, not only for lifetime extension, but also for the cost reduction of the wind power technology [6], [7].

The reliability research in power electronics has been carried out for decades. As the state-of-the-art trend, the reliability engineering in power electronics is now moving from a solely statistical approach that has been proven to be unsatisfactory in the automotive industry, to a more physics-based approach which involves not only the statistics but also the root cause behind the failures [8]–[14]. In this approach, the correct mapping of loading profile which can trigger the failures of components (the stress analysis), as well as the lifetime modeling which investigates how much loading the components can withstand (the strength models), are two of the most important factors for reliability estimation, as illustrated in Fig. 1.

The failure mechanisms of power electronics are complicated and are affected by many factors [19]. It has been revealed that the thermal cycling (i.e., temperature swings inside or outside the devices) is one of the most critical failure causes in power electronics system [11]–[14]. The temperature fluctuation on different materials with mismatched coefficients of thermal expansion may cause disconnection in the contacting areas after certain cycles, thus leading to the failures of the devices. Many manufacturers of power electronic devices such as power semiconductors or capacitors have developed their reliability models, which normally are based on accelerated or aging tests, and are able to transfer certain thermal cycling of components into the corresponding lifetime information [15]–[18]. However, correctly mapping a mission profile of converter into a specific loading profile of power electronic components is a challenging task: For example, in the wind power system, various dynamical changes of wind speeds or ambient temperature at time constants ranging from seconds to months, together with the corresponding control behaviors of turbine, generator, and

Manuscript received August 21, 2013; revised December 3, 2013 and February 20, 2014; accepted March 10, 2014. Date of publication March 18, 2014; date of current version October 7, 2014. Recommended for publication by Associate Editor Y.-M. Chen.

The authors are with the Department of Energy Technology, Aalborg University, Aalborg 9220, Denmark (e-mail: kema@et.aau.dk; mli@et.aau.dk; fbl@et.aau.dk; tak@et.aau.dk).

Color versions of one or more of the figures in this paper are available online at http://ieeexplore.ieee.org.

Digital Object Identifier 10.1109/TPEL.2014.2312335

0885-8993 © 2014 IEEE. Translations and content mining are permitted for academic research only. Personal use is also permitted, but republication/redistribution requires IEEE permission. See http://www.ieee.org/publications_standards/publications/rights/index.html for more information.

converter, all lead to complicated loading profiles of the devices that are difficult to be handled when doing lifetime calculation.

Some simplified methods for the loading profile mapping have been used in traction and electric vehicle applications—they typically focus on a selected and tough operating condition of the converters in a very short term, and then the longer term loading profiles are generated by simply repeating the results acquired in short term [16], [19]–[21]. However, this approach may lead to significant deviation from reality in applications with more complicated mission profiles. For example, in the wind power converter the thermal loading of the power devices does not periodically repeat but randomly changes with the wind speeds and ambient temperature. Moreover, these existing lifetime estimations can just acquire very general lifetime information of devices (e.g., number of years to failure), while the lifetime distribution—which indicates the failure contribution by different loading conditions as well as failure mechanisms, would be more useful for the design and improvement of converter reliability.

In this paper, a more advanced approach for thermal profile mapping as well as lifetime estimation of wind power converter is proposed. It is based on the failure mechanism of power semiconductor devices, i.e., thermal stress generation and lifetime models, and a more complete mission profile of wind power converter are processed considering different time constants. In the end some possibilities as well as limits of the proposed methods are discussed, and some experimental validations regarding the thermal loading of the power devices are given.

II. Basic Idea and Mission Profile for Study

As mentioned earlier, correct transforming the mission profile of wind power converter into the corresponding loading profile of the power devices is a challenging task: First, many factors which have influence on the thermal loading of devices should be taken into account, like the wind speed and ambient variations, behaviors of mechanical parts, behaviors of electrical parts, and also grid conditions. These considerations may involve multidisciplinary models with quite different time constants, and therefore it is difficult to evaluate these models together at the same time step in order to acquire the interested thermal behaviors. Second, in the case of long-term analysis, e.g., 1-year operation which is necessary for lifetime estimation, a large amount of loading data may be generated, which is difficult to be handled if considering too many details of the system. On the contrary, if too rough models and longer time step are used, the generated loading profile may not contain enough thermal dynamics and the lifetime information may significantly deviate from the reality. Therefore, it is important first to develop a way to properly extract and sort the thermal loading in wind power converter for the sake of lifetime estimation.

Inspired by the approach used in photography, where lenses with different focal length are widely used to acquire the images with different sizes and details, the thermal behaviors of the power device in wind power converter can be also focused at different "focal length," which in this case is represented by time constants or time step. According to the main causes of loading change in a wind power converter, the thermal behaviors of power electronic components can be generally classified into three time constants: long term, medium term, and short term, as indicated in Fig. 2. It is noted that in each of the time constant the interested loading behaviors, time step and model details are different, thereby the thermal loading of components can be more efficiently generated. After the loading profiles in each of the time domain are acquired, the corresponding lifetime performance can be estimated, respectively, and then be combined together according to the Miner's rule [22].

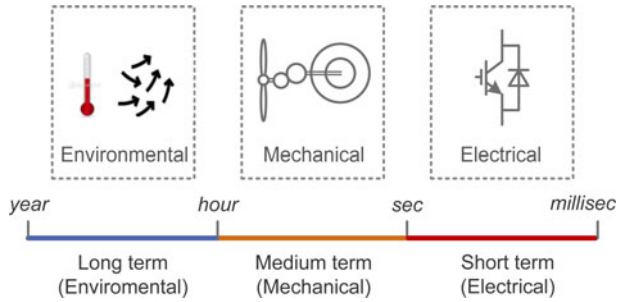

Fig. 2. Thermal cycles of power semiconductors in a wind power converter with three different time constants.

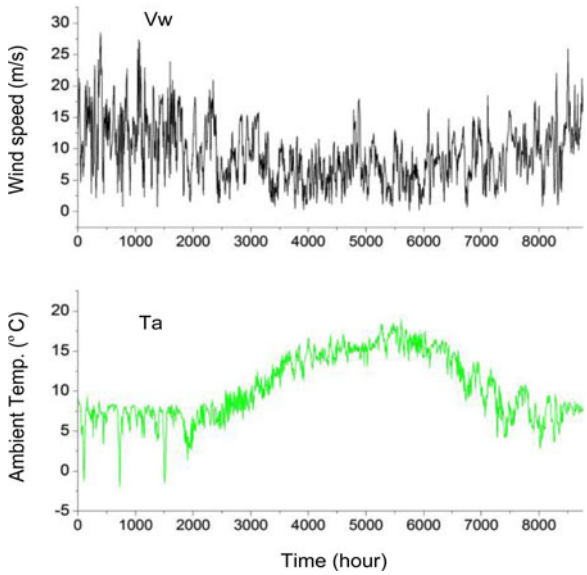

Fig. 3. One year mission profile of wind speed and ambient temperature from a wind farm (3-h averaged).

A typical wind condition and wind turbine system has to be settled first as a study case. As shown in Fig. 3, a 1-year wind speed and ambient temperature profile is used with 3 h averaged at 80 m hub height, which were collected for the wind farm located near Thyborøn, Denmark, with latitude 56.71° and longitude 8.20°. The chosen hub wind speed belongs to the wind class IEC I with average wind speed of 8.5–10 m/s [23], [24] and a 2.0 MW wind turbine V80 [25] is chosen to fit the given wind condition.

In respect to the wind power converter, the most adopted two-level back-to-back voltage source converter topology is chosen, as shown in Fig. 4. Only the grid side converter is chosen as a

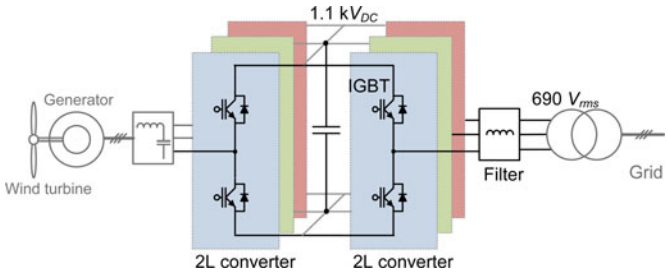

Fig. 4. Wind power converter for lifetime estimation.

TABLE I.
PARAMETERS OF CONVERTER IN FIG. 4

Rated output active power P_o	2 MW
DC bus voltage V_{dc}	1.1 kV DC
*Rated primary side voltage V_p	690 V rms
Rated load current I_{load}	1.93 kA rms
Fundemental frequency f_o	50 Hz
Swtiching frequency f_c	1950 Hz
Filter inductance L_f	132 μH (0.2 p.u.)

*Line-to-line voltage in the primary windings of transformer.

Fig. 5. Flowchart for lifetime estimation of power devices caused by long-term thermal cycles.

case study, whose parameters are basically designed according to Table I, which is a state-of-the-art configuration for the two level wind power converter [1], [3]. The generator side converter can share the similar approach for the analysis.

III. LONG-TERM LOADING PROFILES AND LIFETIME ESTIMATION

As indicated in Section II, the lifetime estimation of wind power converter is going to be conducted under different time constants. In this section, the condition with long-time constant will be analyzed. It is noted that this group of models and estimations only focus on the long-term thermal behaviors and corresponding lifetime caused by the environmental disturbances, e.g., the variation of wind speeds or the ambient temperatures in a few days or months. Therefore, the simplified models and large time step are generally used.

As shown in Fig. 5, the flow for the lifetime estimation under long-term time constant is straightforward: the wind profiles in Fig. 3 is directly fed into a series of wind turbine models in order to generate the corresponding thermal loading of the power devices. Then the acquired thermal loading is processed for lifetime estimation. The analysis in this section is conducted with a time span of 1 year and step of 3 h, which is synchronized with the wind speed and ambient temperature profiles given in Fig. 3.

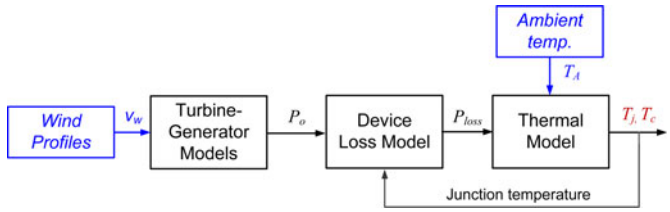

Fig. 6. Multidomain models used for thermal profile generation of power devices.

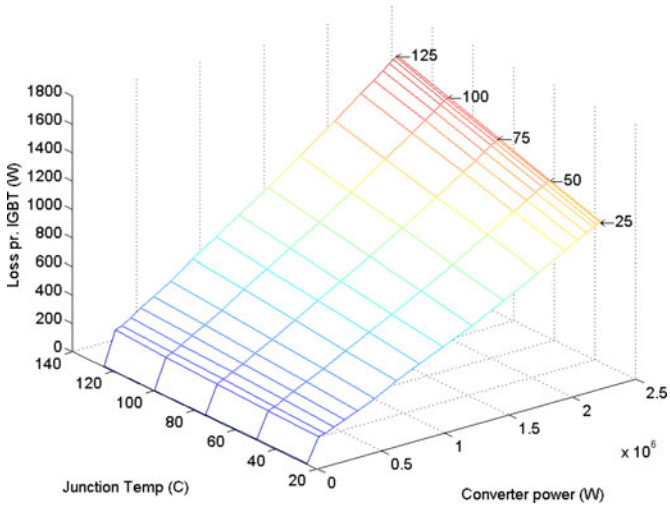

Fig. 7. Three-dimensional lookup table for the IGBT loss in the given wind power converter.

A. Long-Term Loading Profile Generation

In Fig. 6, a diagram for long-term loading profile generation is indicated. It can be seen that multidisciplinary models like the wind turbine, generator, converter, as well as loss and thermal characteristics of the power devices are all included in order to map the mission profile of the wind turbines into the thermal loading of power semiconductors.

Because the wind speed is sampled at 3 h and only long-term thermal behaviors are focused, the inertia effects of the wind turbine and generator which normally range in the time constant of seconds to minutes can be ignored. The output power of wind turbine can be looked up from the power curve provided by the manufacturer [25] and can be directly used as the delivered power of converter.

Similarly, because the response time of converter power and corresponding losses is much smaller than the interested time constant, the loss on the power semiconductor can be directly acquired from lookup table in order to accelerate the analyzing speed. The IGBT module from ABB 5SNA 2400E170305 (2.4 kA/1.1 kV/150 °C) are chosen as power semiconductor devices, which in this paper have maximum junction temperature at 115°C, when the liquid temperature of water-cooled heat sink is at 40 °C. In order to enable the temperature dependence of the device losses [26], [27], a 3-D lookup table is established. As shown in Fig. 7, the losses consumed by the power devices are decided by the input power of converter as well as device junction temperature. For the sake of accuracy, each of the point

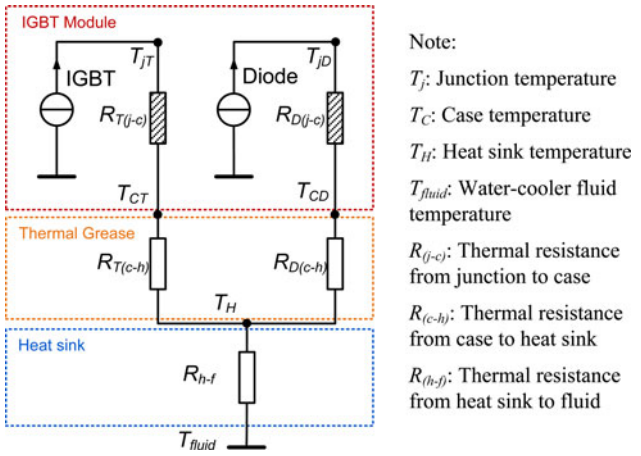

Fig. 8. Thermal network of power semiconductor devices for the long-term thermal profile generation.

in the lookup table is simulated in a detailed circuit model with complete switching behaviors of the power devices, and the conduction loss, switching loss, and diode reverse recovery loss are all taken into account [26].

The thermal model (i.e., the network of thermal resistance and capacitance), which can transfer the acquired power loss in Fig. 7 to the corresponding temperature inside and outside the power devices, is an important consideration for the loading profile generation. Normally, the thermal capacitance of materials will lead to fast thermal changes of the power devices range in the time constants of seconds to minutes [28]—which are still much smaller than the interested time constants for long-term thermal loading. As a result, the thermal capacitance inside the power device as well as the heat sink can be ignored and only thermal resistance is taken into account for long-term loading analysis. The used thermal network is shown in Fig. 8. It is noted that the fluid temperature of the water cooled heat sink T_{fluid} is assumed to be maintained at 40°C if the IGBT is generating power losses, and T_{fluid} is set to the nacelle temperature if the wind speed is below the cut in speed more than12 h.

Based on the aforementioned models and the 1-year mission profile shown in Fig. 3, the long-term thermal loading of the IGBT modules in the given wind power converter can be generated. As shown in Fig. 9, the junction temperature T_j of the IGBT chips, and case temperature T_c of IGBT-based plate are shown respectively because they are closely related to the major failure mechanisms of the IGBT module [16]. It can be seen that the fluctuation of T_j and T_c are very intensive with large fluctuating amplitude from 1-year point of view.

B. Lifetime Estimation With Long-Term Thermal Loading

After the long-term thermal loading of the given IGBT is generated, a rain flow counting method [29], [30] has to be applied in order to convert the randomly changed thermal profile to the regulated thermal cycles which are more suitable to be utilized by the lifetime models. It is becoming a common agreement that not only the amplitude ΔT_j and the mean value T_{jm} of thermal cycles, but also the cycling period t_{cycle} all have strong impacts

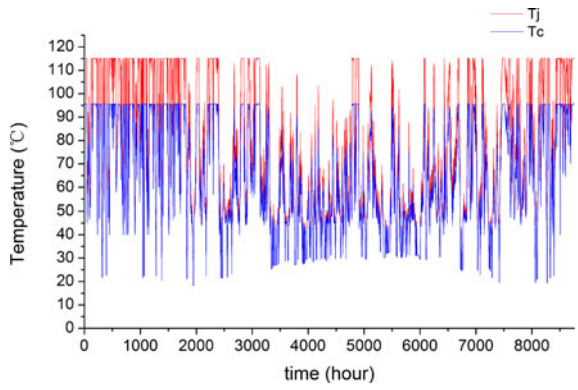

Fig. 9. One year thermal profile under the given mission profile in Fig. 3 (junction temperature T_j and case temperature T_c of the IGBT, time step of 3 h).

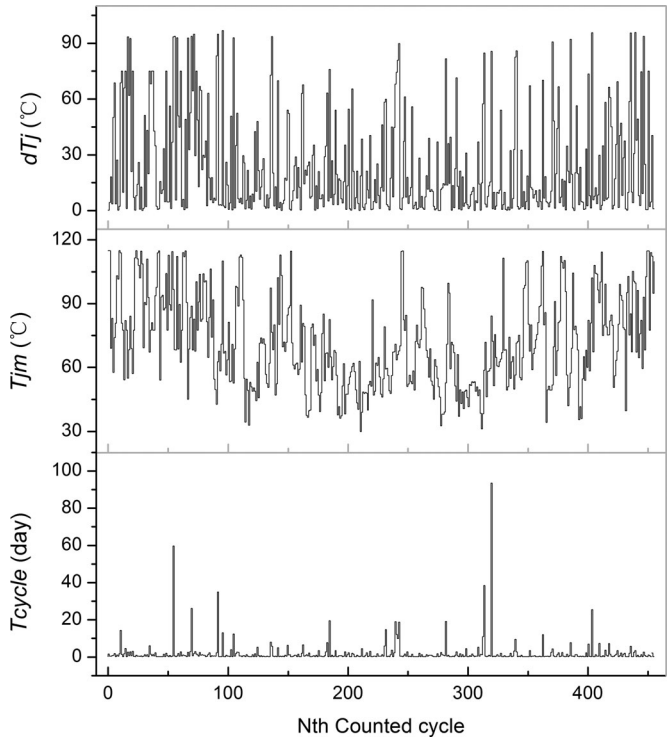

Fig. 10. Rain flow counting results of the junction temperature profile shown in Fig. 9.

to the lifetime of power devices [15]–[18]. Different from the traditional approach, a rain flow counting method which extracts ΔT_j, T_{jm}, and also t_{cycle} is used in this paper. The counting results from the long-term thermal loading in Fig. 9 is shown in Fig. 10, where 460 thermal cycles are identified and each counted cycle with its corresponding ΔT_j, T_{jm}, and t_{cycle} are shown.

After the thermal profiles are counted and regulated, the lifetime models for power devices can be used. There are many different approaches for lifetime modeling of power semiconductor devices, but they are not concluded yet and updated regularly [17], [18]. Generally, the lifetime models provided by device manufacturers are more frequently used. These lifetime models are based on mathematical fitting of enormous aging

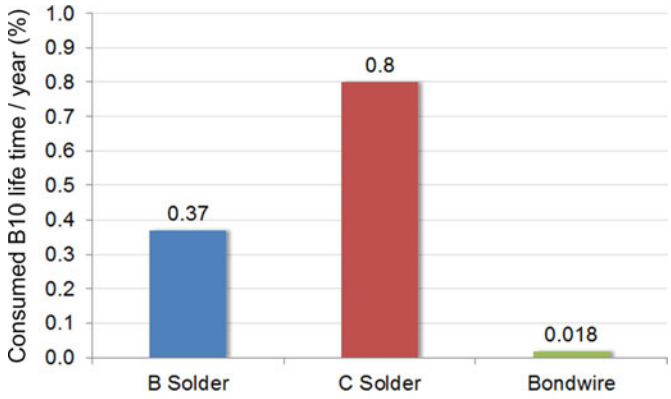

Fig. 11. Consumed B_{10} lifetime of IGBT by long-term thermal cycles for 1 year (lifetime models from [16] is used, only considering thermal cycles ranging from 3 h to 1 year, B solder means base plate solder, C solder means chip solder).

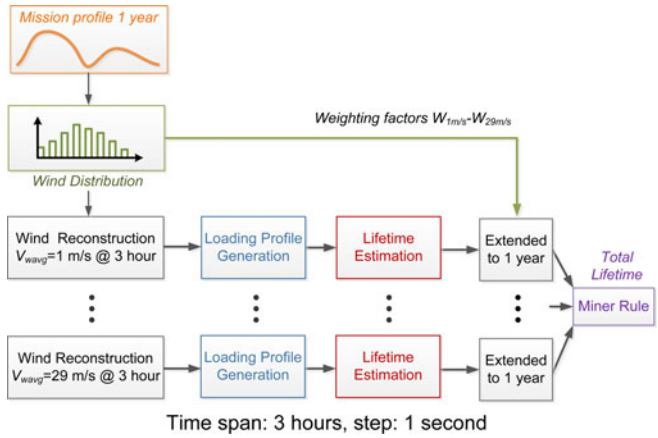

Fig. 12. Flowchart for lifetime estimation of power devices caused by medium-term thermal cycles.

test data, and normally the numbers of thermal cycles N_{life} to a certain failure rate (B_X) is used as an indicator for the lifetime of power devices, which means an individual power device will have $X\%$ probability to fail (or a group of power devices have $X\%$ population to fail) after suffering N_{life} of the thermal cycles.

In this paper, the lifetime model provided by manufacturer is used for the lifetime estimation [16]. This model is a series of lookup tables which can map the nth counted thermal cycle in Fig. 10, to the corresponding number of cycles that the IGBT have 10% failure rate $(N_{n\_\text{life}}$ at $B_{10})$. Then the "consumed B_{10} lifetime" by each counted thermal cycle can simply be calculated in (1). And the total "consumed B_{10} lifetime" by the counted 460 long-term thermal cycles in 1-year $CL_{1\text{year\_long}}$ can be accumulated in (2) according to Miner's rule [22]

$$CL_n = \frac{100}{N_{n\_\text{life}}}(\%) \tag{1}$$

$$CL_{1\text{year\_long}} = \sum_{n=1}^{460} CL_n. \tag{2}$$

The total 1-year consumed B_{10} lifetime of the IGBT module when applying the long-term thermal loading in Fig. 9 are shown in Fig. 11, in which three failure mechanisms like the crack of base plate soldering (B solder, caused by case temperature cycling), crack of chip soldering (C solder, caused by junction temperature cycling), and bond wire lift-off (bond wire, caused by junction temperature cycling) are shown, respectively. It can be seen that the temperature cycling on the chip soldering (C solder) consume more lifetime (i.e., more quick to failure) than the other two failure mechanisms. It is worth to mention that this lifetime result only reflects the influenced by long-term thermal cycles with a period larger than 3 h.

IV. Medium-Term Loading Profiles and Lifetime Estimation

In order to estimate the converter lifetime influenced by the thermal cycles less than 3 h, the loading profile with time constants of seconds to minutes has to be established. This group of analysis mainly focuses on the medium-term thermal loading

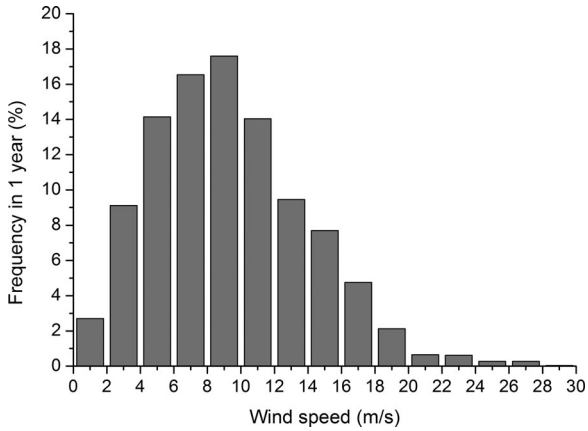

Fig. 13. Speed distribution of the given wind profile shown in Fig. 3 (scaled at 2 m/s step).

of power device caused by the mechanical behaviors of wind turbine system, such as the pitch control to limit the generated power and speed control to maximize the power production. Therefore, more complicated models and smaller time step have to be applied in order to generate enough details of the loading information and thus correctly estimate the lifetime. In this section, the analysis is conducted with time span of 3 h in order to restrain the data size, and a time step of 1 s is applied. However, the loading profile of 3 h only accounts for a small part of the complete loading information in 1 year, which is necessary for the lifetime estimation of power devices. As a result, an extrapolation method from 3 h to 1 year has to be proposed.

As shown in Fig. 12, the flow for lifetime estimation caused by medium-term thermal loading is different from Fig. 5: the wind profile in Fig. 3 is first converted to a wind speed distribution, as indicated in Fig. 13, which represents the frequency of a certain wind speed appearing in 1 year (% in 365 days). Afterward a series of wind speed variations within 3 h are reconstructed. The used model for wind speed generation has been developed at RISØ National Laboratory based on the Kaimal spectra [31]. The wind speed is calculated as an average value over the whole rotor, and it takes the tower shadow and the rotational turbulences into account. A turbulence intensity of 18% is

applied, which belongs to the Class A wind turbulence [23] and is also the defined wind condition by the used wind turbines. Then the rotor rotational speed and the desired average wind speed are the two inputs for the wind speed generation model. As an example shown in Fig. 15, three generated wind speed variations within 3 h at average speed of 7, 11, and 23 m/s are illustrated.

By processing each of the reconstructed wind speed variations of 3 h at different average values $V_{\rm ave}$, the loading profiles generations as well as the lifetime estimations are implemented, respectively, and then the total 1-year consumed lifetime by medium-term thermal cycles can be extrapolated by including the information of wind speed distribution. More details of the process are demonstrated as follows.

A. Medium-Term Loading Profile Generation

Because the interested time constant for the medium-term thermal loading is reduced to seconds' level, the dynamics of the mechanical parts cannot be ignored. In order to focus the analysis on the converter loading and lifetime estimation, an inertia transfer function with time constant of 20 s is added to roughly emulate the power inertia of the wind turbine, drive train, and generator. Nevertheless the used models can be further detailed depending on the required accuracy.

Moreover, the turn ON and turn OFF of power converter will introduce significant power changes and thus have strong effects on the thermal cycling of power devices; therefore, the cut-in and cut-out behaviors of wind turbine should be carefully specified for lifetime estimation. According to the datasheet, it is defined that the rated wind speed for the used wind turbine is at 12 m/s. The cut-in wind speed is set at 3 m/s with 5 min average, cut out wind speed is at 25 m/s with 5 min averaged or 32 m/s with 5 s averaged. The recut in wind speed is set at 24 m/s with a delay time of 30 min to emulate the startup process of the whole wind power generation system. Based on the assumed behaviors of wind turbines, three output power of wind power converter are shown in Fig. 15, where the conditions when the average wind speed $V_{\rm ave} = 7$, 11, and 23 m/s are illustrated, respectively.

In this section, the interested thermal behaviors of power devices have much smaller time constant, therefore the thermal capacitance which determines the fast thermal dynamics ranging from seconds to minutes can no longer be ignored. Unfortunately, as detailed in [32], it is found that both of the existing Cauer and Foster thermal networks which contain thermal capacitance have their limits to acquire the appropriate case temperature of power device. As a result, a new thermal model which combines the advantages of these two thermal networks is proposed [32]. As shown in Fig. 14, the proposed thermal model contains two paths, and it is noted that to ensure a mathematically correct model, the heat flow in these two thermal paths are not coupled: The first thermal path is used for the junction temperature estimation. In this path, the datasheet-based multilayer Foster thermal network inside power devices are used, and only a temperature potential, whose value is determined by the case temperature T_c from the other thermal path, is connected to the Foster network. As a result, the Foster network

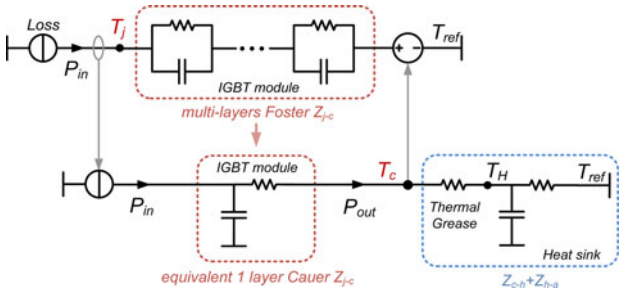

Fig. 14. Thermal network of power semiconductor devices for the medium-term thermal loading generation (only the thermal path of IGBT is illustrated for simplicity, $T_{\rm ref}$ means the reference temperature for the fluid or ambient of heat sink).

is correctly used and abrupt change of case/junction temperature can be avoided [32]. The second thermal path is used for the case and heat sink temperature estimation. In this path, the thermal network inside IGBT module is just used for the loss filtering rather than for the junction temperature estimation, and the complete thermal network outside the IGBT module (i.e., thermal grease and heat sink) have to be included. It is noted that the multilayer Foster network inside the IGBT module is mathematically transformed to a single-layer Cauer RC unit. This transformation will lose some accuracy for the thermal dynamics of junction temperature, but it can regain certain physical meaning because any object can be simply represented as a single Cauer RC unit from the thermal point of view; therefore, it is more suitable for the loss filtering and establishment of the case temperature T_c, which has much slower thermal dynamics than the junction temperature T_j [32].

By the proposed thermal model and simulation method, it is possible to estimate not only the junction temperature but also the case and heat sink temperature in a relative long-time period. When feeding the input power of converter in Fig. 15 to the loss and thermal model of the devices shown in Figs. 7 and 14, the medium-term thermal loading of the IGBT (T_j and T_c) can be generated, as shown in Fig. 16. It can be seen that the medium-term thermal behaviors of power devices have several notable features: Generally the T_j is higher than T_c and has faster thermal dynamics. Both T_j and T_c fluctuate accordingly with the output power of converter with much smaller fluctuating amplitude compared to the long-term thermal profile in Fig. 9. Moreover, the thermal loadings of power devices are quite different under various wind conditions, when average wind speed is below 11 m/s, the fluctuation amplitude of T_j and T_c increases with the increasing of wind speeds, as shown in Figs. 16(a) and 16(b); when the average wind speed is higher than 11 m/s, the temperature fluctuation is much smaller, and the cut-out and recut-in behaviors of wind turbine will introduce significant thermal cycles to the power devices, as shown in Fig. 16(c).

B. Lifetime Estimation With Medium-Term Thermal Loading

With the same approach used in Section II to count and convert the thermal loadings in Fig. 16, the consumed lifetime of power device by medium-term thermal cycles can be estimated.

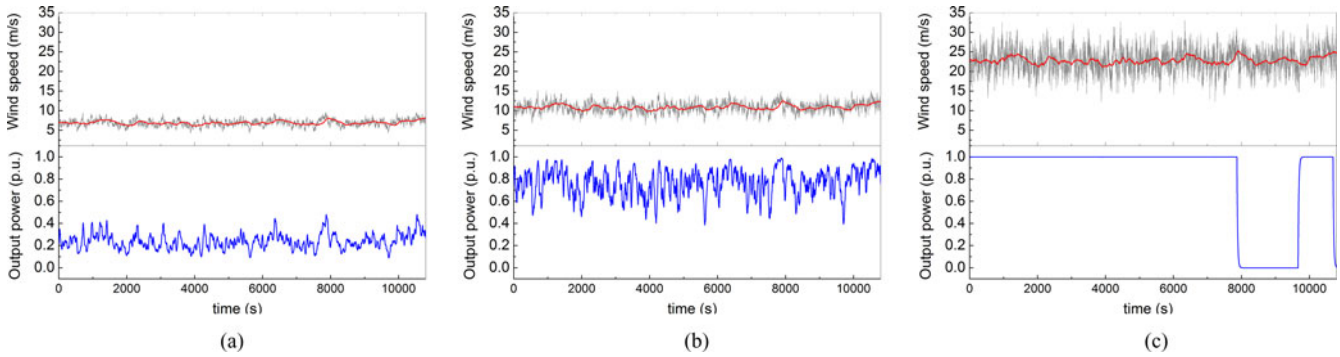

Fig. 15. Generated wind speeds (instantaneous and 3-min averaged) and corresponding output power of wind turbine (3 h with 1 s time step, turbulence intensity of 18%). (a) $V_{\rm ave} = 7$ m/s. (b) $V_{\rm ave} = 11$ m/s. (c) $V_{\rm ave} = 23$ m/s.

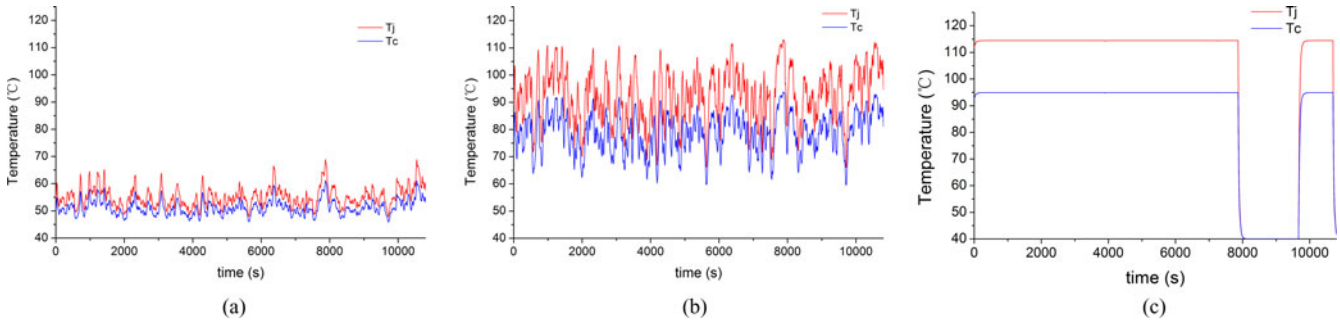

Fig. 16. Medium-term thermal loading of IGBT when applying the wind profiles in Fig. 15 (3 h with 1 s time step). (a) $V_{\rm ave} = 7$ m/s. (b) $V_{\rm ave} = 11$ m/s. (c) $V_{\rm ave} = 23$ m/s.

In order to extrapolate the lifetime results from 3 h to 1 year, the thermal generation and lifetime estimation are carried out 15 times under each wind speed variation of 3 h with different $V_{\rm ave}$ (from 1 to 29 m/s with step of 2 m/s). Then the 1-year total consumed lifetime by medium-term thermal loading can be accumulated with

$$CL_{1\,\text{year\_medium}} = \frac{365 \cdot 24}{3}(W_{1\,\text{m/s}} \cdot CL_{1\,\text{m/s\_3 h}} + W_{3\,\text{m/s}} \cdot CL_{3\,\text{m/s\_3 h}} + \cdots + W_{29\,\text{m/s}} \cdot CL_{29\,\text{m/s\_3 h}}) \quad (3)$$

where $W_{1\,\text{m/s}}$ to $W_{29\,\text{m/s}}$ are the weighting factors obtained from the density of wind speed distribution in Fig. 13.

The calculated 1-year consumed B_{10} lifetime of the IGBT module when applying the given medium-term thermal loadings are shown in Fig. 17, in which the consumed lifetime by three failure mechanisms are given, respectively. It is noted that this consumed lifetime only reflects the impacts by medium-term thermal cycles with period between 1 s to 3 h. Different from Fig. 11, the temperature cycling on the based plate of IGBT consumes more lifetime than the other two failure mechanisms.

By the proposed approach for lifetime estimation caused by medium-term thermal loading, another interesting lifetime information can be plotted in Fig. 18 as function of wind speeds. It can be seen that the lifetime of the power devices is consumed intensively at wind speeds of 10–12 m/s. This speed range is around the rated wind speed of the wind turbine, when the pitch system of wind turbine need to be activated and the output power of the converter varies significantly, as it can be observed in Fig. 15(b).

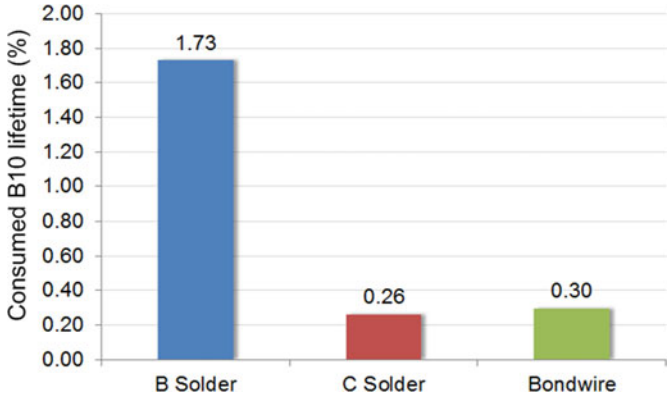

Fig. 17. Consumed B_{10} lifetime of IGBT by medium-term thermal cycles for 1 year (lifetime models from [16] is used, only considering the thermal cycles ranging from 1 s to 3 h, B solder means base plate solder, C solder means chip solder).

V. Short-Term Loading Profiles and Lifetime Estimation

In order to estimate the converter lifetime influenced by the short-term thermal cycles with less than 1 s, the loading profile with time constants of milliseconds has to be established. This group of thermal behavior is mainly caused by the fast electrical disturbances of the converter such as load current alternating, switching of power device, or the impacts of grid faults. Therefore, small time steps are generally required for analysis.

As it is difficult to investigate the complete loading profile of 1 year with the required small time step, the idea for lifetime

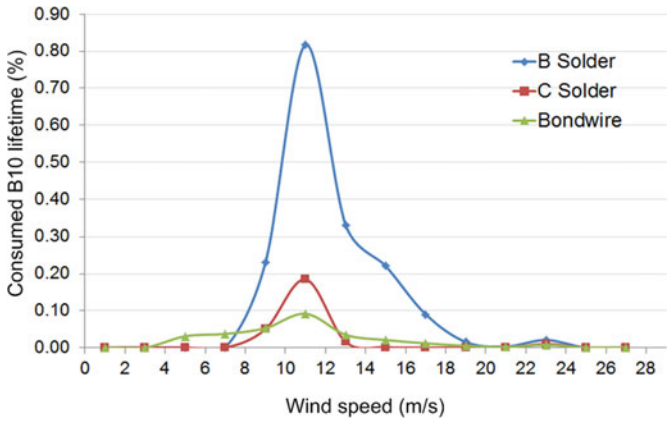

Fig. 18. Consumed B_{10} lifetime distribution by medium-term thermal cycles (lifetime models from [16] is used, only considering the thermal cycles ranging from 1 s to 3 h, B solder means base plate solder, C solder means chip solder).

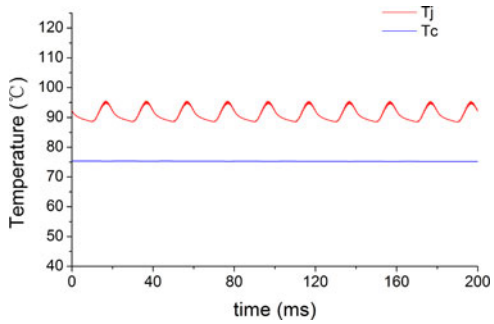

Fig. 19. Short-term thermal behaviors inside power device when wind speed $v_w = 12$ m/s (0.2 s with 0.5 ms time step, $T_{\rm ref} = 40°$C).

estimation and extrapolation as shown in Fig. 12 is also applied for the lifetime analysis with short-term thermal loadings. However, the methods for loading profile generation and used lifetime models are different, as explained in the following.

A. Short-Term Loading Profile Generation

This group of thermal behaviors in the power devices is mainly caused by the fast and periodical current alternating in the converter. The junction temperature of power devices swings at relative smaller amplitude and at fundamental frequency of the converter output. A simulation result is shown in Fig. 19, where the converter is operating under rated condition of Table I, and the T_j and T_c within 200 ms are illustrated. It can be seen that the junction temperature T_j oscillates at 50 Hz with constant swinging amplitude, while the case temperature T_c remains almost unchanged. Therefore, with the information of temperature mean value and cycling amplitude, the lifetime models can be directly applied to T_j without rain flow counting. And because of relative larger thermal capacitance, the thermal dynamics of the T_c is not as fast as the T_j, thereby the case temperature are not considered in the lifetime estimation by short-term thermal cycles.

As detailed in [34], the cycling amplitude of the junction temperature ΔT_j caused by load current altering of converter can be analytically solved by

$$\Delta T_j = P_{\rm loss} \cdot Z_{\rm th}\left(\frac{3}{8f_o}\right) + 2P_{\rm loss} \cdot Z_{\rm th}\left(\frac{1}{4f_o}\right) \quad (4)$$

where $P_{\rm loss}$ is the loss of power device which can be looked up from Fig. 7; $Z_{\rm th}$ is a time-based expression of device thermal impedance, which can be found in the datasheet; f_o is the fundamental frequency of the converter output, which is normally set at 50 Hz and it is also the cycling frequency of the interested thermal behavior in short term.

In respect to the mean junction temperature, the loading profile shown in Fig. 16 can be directly used. Therefore, the generation of short-term loading profile can be significantly accelerated because the detailed circuit models with the switching behaviors can be avoided, and only analytical functions of (4), as well as a series of simulations with medium time step are needed.

B. Lifetime Estimation With Short-Term Thermal Loading

It is noted that due to the lack of the testing data, most manufacturer cannot provide enough lifetime information by thermal cycles with small ΔT_j ($<$10 K) and high cycling frequency ($>$1 Hz). The manufacturer has a Coffin–Manson-based lifetime model [35] which is tested under cycling period of 2 s, this is the closest testing condition that can be found and it is used in this paper for a rough approximation. The lifetime model can be expressed as

$$N_{\rm life} = 1.017^{(125-T_{j\rm m}-\Delta T_j/2)^{1.16}} \times 8.2 \cdot 10^{14} \times (\Delta T_j)^{-5.28}. \quad (5)$$

It is noted that this lifetime model only reflects the general failures of IGBT module and cannot separate the three failure mechanisms shown in Fig. 11. When inputting the mean junction temperature T_{jm} from Fig. 16, and ΔT_j from (4), the consumed lifetime of IGBT caused by the short-term thermal cycles (50 Hz) can be mapped. It is noted that in order to extrapolate the lifetime results from 1 s to 1 year, the simulations are carried out 15 times under 3 h medium-term wind profiles with different average speeds (1, 3, 5, . . .,29 m/s). Then the total consumed lifetime in 1 year can be accumulated according to the wind speed distribution shown in Fig. 13.

The 1-year lifetime distribution of IGBT under different wind speeds by short-term thermal cycles is shown in Fig. 20. It is interesting to see that the lifetime is consumed intensively at wind speeds of 14–15 m/s, this is quite different from the lifetime distribution by the medium-term thermal cycles shown in Fig. 18, where the lifetime is consumed intensively at 10–12 m/s. This is because the cycling amplitude of short-term thermal loading is mainly decided by the absolute power loss which achieves the maximum at 14–15 m/s when the wind turbine generates the maximum output power. It is noted that in Fig. 20 the values of consumed lifetime is much higher than the one shown in Fig. 18, this is because different lifetime models are used and the number of thermal cycling is significantly larger in short-term thermal behaviors.

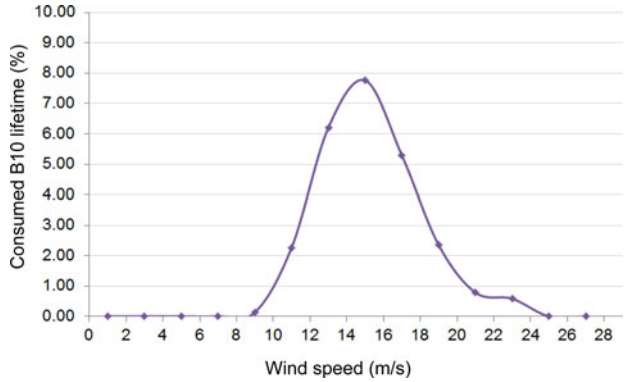

Fig. 20. Consumed B_{10} lifetime distribution by short-term thermal cycles (lifetime models from [35] is used; only thermal cycles below 1 s are considered).

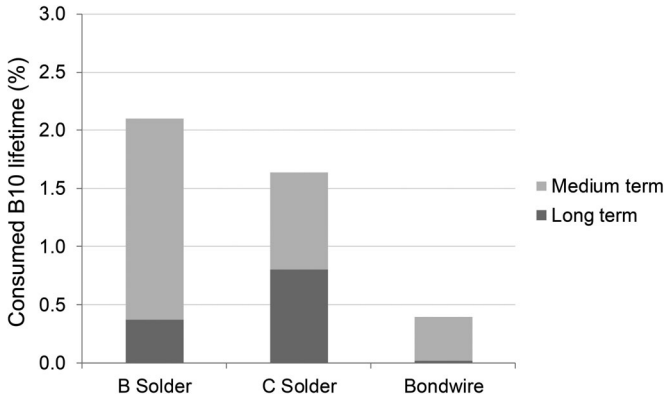

Fig. 21. Total 1-year consumed lifetime distribution by different failure mechanisms and thermal behaviors (lifetime models from [16] is used).

VI. Possibilities and Limits Discussion of the Proposed Method for Lifetime Estimation

With the proposed lifetime estimation approach for wind power converter, some other interesting information related to the lifetime of power devices can be acquired. Fig. 21 shows the consumed lifetime distribution by different failure mechanisms as well as the thermal behaviors under different time constants. Among medium-term and long-term thermal cycles, the critical thermal stresses which cause the reliability problem of the given converter can be addressed—the base plate and chip solder fatigues caused by medium-term thermal cycles. Because the used lifetime model in Fig. 21 only covers thermal cycles with very limited cycling period (10 s–1 day), the lifetime consumed by short-term thermal cycles (1 s below) is not applicable and thereby is not included.

Fig. 22 shows a series of consumed lifetime distribution at different wind speeds caused by medium-term and short-term thermal cycles, where the same loading profiles of power devices are applied with another important lifetime model from [15] and [17]. It is noticed that because this lifetime models only covers the thermal cycling at period between 2 and 30 s, the long-term thermal loadings are not included. It is noticed that different lifetime models mentioned in this paper are developed based on various technologies, ratings, testing conditions and the criteria of failures, thereby the acquired lifetime when different

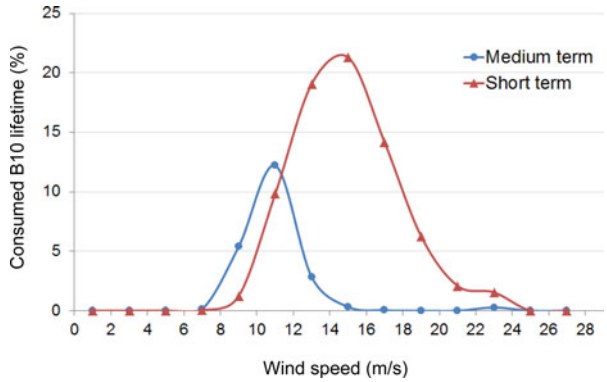

Fig. 22. Consumed lifetime distribution of IGBT by medium- and short-term thermal cycles (lifetime model from [15], [17]).

models are applied may vary in a large range even with the same loading of power device; however, the justification and evaluation of these lifetime models are out of the scope of this paper which mainly focuses on how to use them.

It is worth to mention that most of the lifetime models provided by manufacturer are based on accelerated tests, which can only cover very limited ranges of ΔT_j, T_{jm}, and t_{period} of the thermal cycles because the accelerated tests are very time consuming. Moreover, some testing conditions are relative hard to be implemented such as very fast or very slow thermal cycling, or cycling with low T_{jm} but large ΔT_j [15]–[17]. However, in this paper, it was found that in the wind power applications many thermal behaviors the power devices will present, which are not yet tested to map the corresponding lifetime. In this paper, in order to translate these "unidentified thermal cycles" into lifetime, ΔT_j and T_{jm} are interpolated/extrapolated linearly with log scale, and some cycling period t_{period} are not consistent with the specification in the lifetime models—-this could lead to in-confidence of the acquired lifetime results. Therefore, even more advanced lifetime models which can cover more loading conditions of power devices are required for better lifetime estimation based on mission profiles.

Furthermore, it is noted that the three time intervals and corresponding time steps in Sections III–V are qualitative definitions, which give emphasis on separating the analysis at different time scale and details of the models. Depending on the study cases, the used models, available data, and needs of accuracy, the specific time intervals and steps can be varied. However, the basic idea and approach for the lifetime estimation can be generally adapted to different scenarios, where the long, medium, and short term can be defined individually.

It is also noted that the failure mechanisms of power electronics are complicated and are related to many factors [36]–[41]. In this paper, the fatigue on the interconnections inside IGBT modules based on soldering and aluminium bond wires is mainly focused, and according to many surveys the thermal cycling is one of the most important causes of failure for this failure mechanism. However, in respect to other cause of failures in power electronics like electrical degradation, humidity, vibration, cosmic radiation, etc., quite different scenarios and approaches have to be involved and they cannot be evaluated in this paper.

VII. Validation of the Results

A. Discussion on the Lifetime Validation

One potential way to validate the lifetime estimation by this paper is to justify the obtained results with the failure statistics observed in real-world wind power converters. Some comprehensive investigations of the failures in wind power converters were implemented in [4], [5], [42]–[44]. However, these data normally does not reflect the state-of-the-art wind turbine technology and most of them only recorded the numbers of failures for the whole converter system. While more detail information like the causes and types of failures are seldom available or hard to be accessed by the public. As mentioned earlier and also addressed in [2], [19], [36]–[38], thermal-related failures of power semiconductor devices (the focus of this paper) are just one part of the whole reliability calculation for the converter system, therefore the general failure statistics, which include many other unknown causes of failure, cannot be used to validate the thermal-related lifetime modeled in this paper.

Nevertheless, some of the general reliability information obtained by this paper can be partly agreed to by the existing works having different focuses and approaches. In [41] and [45], it was found that the wind power converter consumes the lifetime much more intensively around rated wind speed, this is agreed by the results shown in Fig. 18. In [16] and [18], it was claimed that as the technology improvement, soldering fatigues start to dominate the failures of the IGBT modules instead of bond wire liftoff, this conclusion is consistent with the results shown in Figs. 11, 17, and 21. In [40], Weiss and Eckel point out the small thermal cycles should be also important factor for device failures, this discovery agrees with the results given in Fig. 22.

It is worth to mention that as one of the most important causes of failure in power electronics, thermal loading of power devices should be closely related to the specific mission profiles of the converter [36]–[41]. This correlation has not yet been clearly validated especially when considering different time constants in wind power application. Therefore, the validation of the thermal behaviors caused by the mission profiles under different time constants will be the main target of this paper, because it is a critical step for the lifetime estimation conducted in this paper.

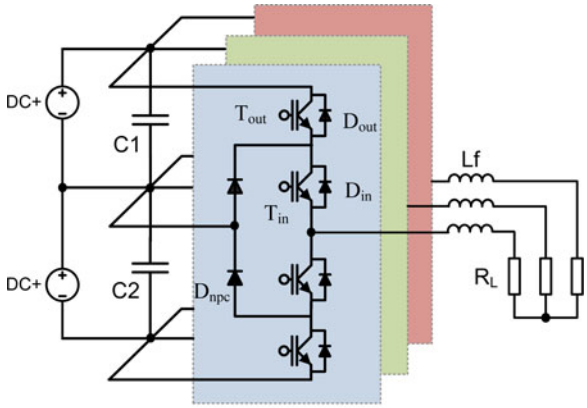

(a)

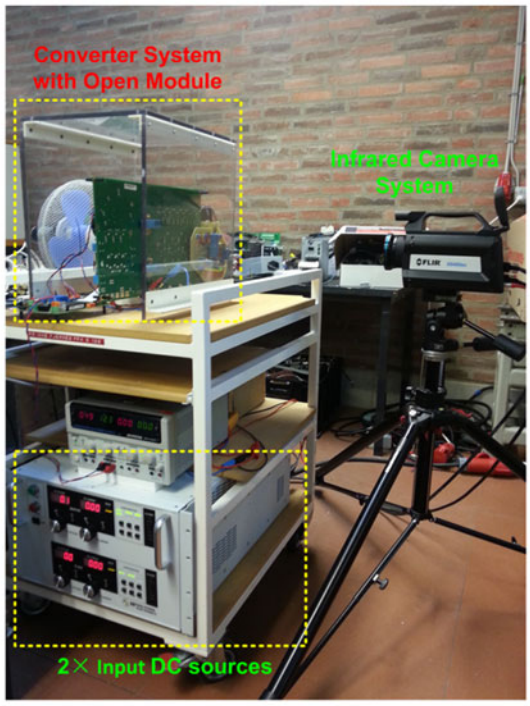

(b)

Fig. 23. Configurations of experimental setup for thermal behavior validation. (a) Circuit topology (3 L-NPC, power module of phase A is opened and black painted). (b) Setup photo (main parts are indicated).

B. Validation of Thermal Loading in Power Device Under Different Time Constants

The thermal behaviors caused by medium- and short-term mission profiles are validated on a downscale dc–ac converter. The approach is to use a high-frequency infrared thermal camera to obverse the internal structure of an opened power module during the operation of converter. As shown in Fig. 23, the circuit configurations and setup photo are both illustrated. A three-phase three-level neutral point clamped converter (3 L-NPC) is used because this topology has only half of the voltage stress on the devices compared to the 2 L converter, and this advantage is beneficial for the long-term operation of the setup because the used power module is opened with degraded voltage insulation capability. The detailed parameters of the experimental setup are shown in Table II. Two dc sources are used to feed the

TABLE II
Parameters of Experimental Setup

DC bus voltage V_{dc}	600 V DC
DC capacitance C_1/C_2	3300 μF
Rated power P_{rated}	10 kW
Max. load current I_{max}	20 A
Fundamental frequency f_o	50 Hz
Switching frequency f_s	20 kHz
Filter inductance L_f	3 mH
Load resistance R_L	16 Ω
Infrared camera	FLIR X8400sc
3L-NPC Power Module	1200 V / 30 A

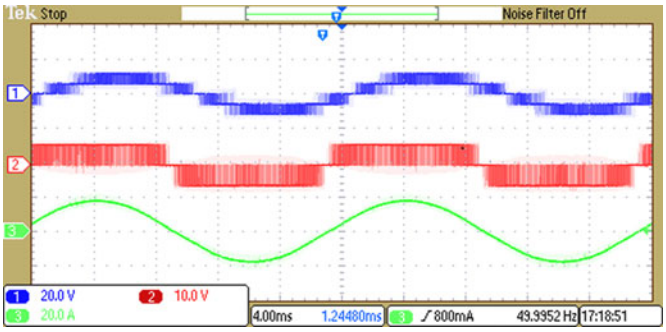

Fig. 24. Electrical outputs of converter setup at rated condition, line-to-line voltage pulses—signal 1 (1 kV/div), phase voltage pulses—signal2 (500 V/div), load current— signal 3 (20 A/div), 4 ms/div, modulation index $M = 1$ p.u., DC bus voltage $V_{\rm dc} = 600$ V, $f_s = 20$ kHz, $PF = 1$.

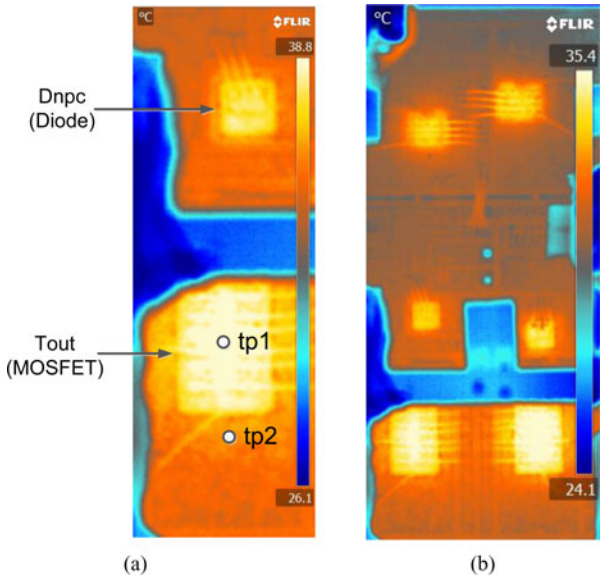

Fig. 25. Thermal image inside a 3L-NPC power module by infrared camera during the operation of converter ($T_{\rm out}$ and $D_{\rm npc}$ chips are indicated, rated operating condition of Fig. 24, data acquisition points are indicated as tp1 (T_j) and tp2 (T_c) in the image, MOSEFET is imaged). (a) Zoom-in on two chips. (b) Overview of the whole module.

converter with constant dc voltage and three-phase passive RL loads are applied, thereby the current loading of device can be adjusted by changing the modulation index. Based on the setup the electrical outputs of converter under rated condition are shown in Fig. 24, where the line-to-line voltage pulses (blue), phase voltage pulses (red), and load current (green) in one phase are indicated, respectively.

A thermal image of the opened power module observed by infrared camera is shown in Fig. 25, where the outer switch chip $T_{\rm out}$ and the clamping diode chip $D_{\rm npc}$ in Fig. 23(a) are illustrated; the converter is operating under the rated conditions given in Table I. As shown in Fig. 25, the temperature distribution on the chips and based plate can be clearly observed, where two testing points tp1 and tp2 are defined to represent the chip temperature T_j and base plated temperature T_c, respectively.

The thermal profiles of the two predefined testing points within a medium term is shown in Fig. 26, in which the current

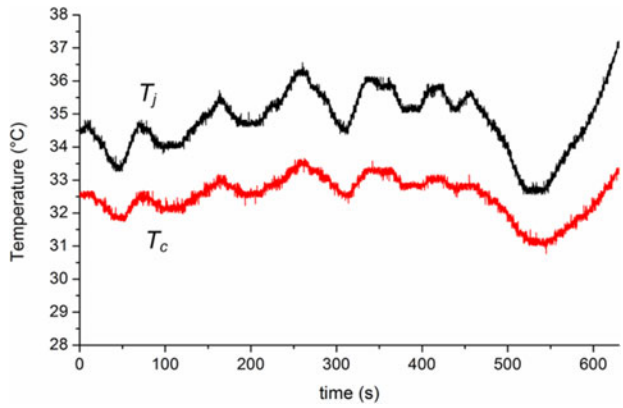

Fig. 26. Experimental results of medium-term thermal behaviors within 10 min (corresponding to segment of 5100–5700 s in Fig. 16 (b), with temperature sampling rate at 10 Hz).

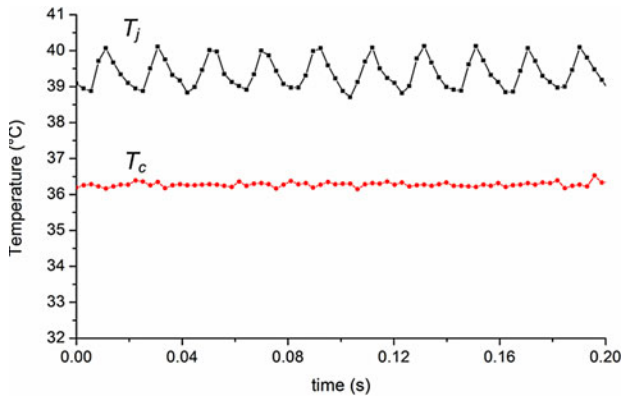

Fig. 27. Experimental results of short-term thermal behaviors within 0.2 s (corresponding to Fig. 19, current loading is maintained constant under rated condition of Table II, with temperature sampling rate at 350 Hz).

loading is varied according to the p.u. converter power within a 10 min segment (5100–5700 s) shown in Fig. 15(b), and the temperature sampling rate by infrared camera is set at 10 Hz. It can be seen that T_j is higher than T_c with larger cycling amplitude, and they fluctuate in accordance with the current loading—these features are consistent with the estimated thermal profiles shown in Fig. 16(b).

The thermal behaviors of the two predefined testing points within a short term is shown in Fig. 27, in which the current loading of converter remains constant at rated output power of 10 kW, and the sampling rate of temperature is set at 350 Hz. It can be seen that the thermal profiles are quite different compared to the one under medium term shown in Fig. 26: T_j oscillates at the fundamental frequency of 50 Hz with constant fluctuating amplitude of 1.5 °C, while T_c is almost constant without significant fluctuations—these features are consistent with the estimated thermal profiles shown in Fig. 19.

VIII. Conclusion

A comprehensive lifetime estimation method for the power semiconductors in wind power converter is proposed in this paper. It is based on the thermal cycling and corresponding strength models inside power devices, and the method separates the

analysis under different time constants of the thermal behaviors in the wind turbine system. With the established approaches for loading profile generation and lifetime estimation, more possibilities and details of the lifetime information for wind power converter can be obtained like the lifetime consumption by different thermal behaviors, wind speeds, and failure mechanisms. This is very useful to indicate and improve the weakness of the system in respect to the reliability performance. The estimated thermal behaviors in the power devices are validated on a downscale experimental setup.

It is also found that in the wind power application, many loading conditions of power devices that are not covered by most of the lifetime models by manufactures could be presented. Therefore, more advanced lifetime modeling and power cycling tests are required for the lifetime estimation of converter based on mission profiles.

REFERENCES

[1] F. Blaabjerg, M. Liserre, and K. Ma, "Power electronics converters for wind turbine systems," *IEEE Trans. Ind. Appl.*, vol. 48, no. 2, pp. 708–719, Mar./Apr. 2012.

[2] F. Blaabjerg and K. Ma, "Future on power electronics for wind turbine systems," *IEEE J. Emerg. Select. Topics Power Electron.*, vol. 1, no. 3, pp. 139–152, Sep. 2013.

[3] Z. Chen, J. M. Guerrero, and F. Blaabjerg, "A review of the state of the art of power electronics for wind turbines," *IEEE Trans. Power Electron*, vol. 24, no. 8, pp. 1859–1875, Aug. 2009.

[4] S. Faulstich, P. Lyding, B. Hahn, and P. Tavner, "Reliability of offshore turbines–identifying the risk by onshore experience," in *Proc. Eur Offshore Wind*, Stockholm, Sweden, 2009, pp. 1–10.

[5] B. Hahn, M. Durstewitz, and K. Rohrig, "Reliability of wind turbines—Experience of 15 years with 1500 WTs," in *Wind Energy*. Berlin, Germany: Spinger, 2007.

[6] Wikipedia. (Apr. 2013). "Cost of electricity by source," [Online]. Avaiable: http://en.wikipedia.org/wiki/Cost_of_electricity_by_source

[7] "Levelized cost of new generation resources in the annual energy outlook 2013," Report of the US Energy Information Administration (EIA) of the U.S. Department of Energy (DOE), DOE/EIA-0383ER, 2013.

[8] C. Byrne, et al., "Handbook for robustness validation of automotive electrical/electronic modules," *ZVEI Zentralverband Elektrotechnik- und Elektronikindustrie e. V.*, Frankfurt, Germany, Jun. 2013

[9] E. Wolfgang, L. Amigues, N. Seliger, and G. Lugert, "Building-in reliability into power electronics systems," *The World Electron. Packag. Syst. Integr.*, pp. 246–252, 2005.

[10] D. Hirschmann, D. Tissen, S. Schroder, and R. W. De Doncker, "Inverter design for hybrid electrical vehicles considering mission profiles," in *Proc. IEEE Conf. Vehicle Power Propulsion*, Sep. 2005, no. 7–9, pp. 1–6.

[11] C. Busca, R. Teodorescu, F. Blaabjerg, S. Munk-Nielsen, L. Helle, T. Abeyasekera, and P. Rodriguez, "An overview of the reliability prediction related aspects of high power IGBTs in wind power applications," *Microelectron. Rel.*, vol. 51, no. 9–11, pp. 1903–1907, 2011.

[12] E. Wolfgang, "Examples for failures in power electronics systems," presented at ECPE Tuts. Rel. Power Electron. Syst., Nuremberg, Germany, Apr. 2007.

[13] S. Yang, A. T. Bryant, P. A. Mawby, D. Xiang, L. Ran, and P. Tavner, "An industry-based survey of reliability in power electronic converters," *IEEE Trans. Ind. Appl.*, vol. 47, no. 3, pp. 1441–1451, May/Jun. 2011.

[14] J. Due, S. Munk-Nielsen, and R. Nielsen, "Lifetime investigation of high power IGBT modules," in *Proc.14th Eur. Conf. Power Electron. Appl.*, Birmingham, England, 2011, pp. 1–8.

[15] A. Wintrich, U. Nicolai, W. Tursky, and T. Reimann, "Application manual Power Semiconductors," in *SEMIKRON International GmbH, Nuremberg, Germany*, 2011, pp. 127-129.

[16] J. Berner, "Load-cycling capability of HiPak IGBT modules," ABB Application Note 5SYA 2043-02, 2012.

[17] U. Scheuermann, "Reliability challenges of automotive power electronics," *Microelectron. Rel.*, vol. 49, no. 9–11, pp. 1319–1325, 2009.

[18] U. Scheuermann and R. Schmidt, "A new lifetime model for advanced power modules with sintered chips and optimized Al wire bonds," in *Proc. Power Electr., Intell. Motion, Renew. Energy and Energy Manag.*, 2013, pp. 810–813.

[19] H. Wang, K. Ma, and F. Blaabjerg, "Design for reliability of power electronic systems," in *Proc. IEEE 38th Annu. Conf. Ind. Electron. Soc.*, 2012, pp. 33–44.

[20] H. Wang and D. Zhou, "A reliability-oriented design method for power electronic converters," in *Proc. IEEE 28th Annu. Appl. Power Electron. Conf.*, 2013, pp. 2921–2928.

[21] O. S. Senturk, S. Munk-Nielsen, R. Teodorescu, L. Helle, and P. Rodriguez, "Electro-thermal modeling for junction temperature cycling-based lifetime prediction of a press-pack IGBT 3 L-NPC-VSC applied to large wind turbines," in *Proc. IEEE Energy Convers. Congr. Expo.*, 2011, pp. 568–575.

[22] M.A. Miner, "Cumulative damage in fatigue," *J. Appl. Mech.*, vol. 12 (trans ASME vol. 67), pp. A159–A164, 1945.

[23] Wikipedia. (2013, Jun). "IEC 61400," [Online]. Avaiable: http://en.wikipedia.org/wiki/IEC_61400#cite_note-woeb-1

[24] Wind Turbines Classes. (2013, Jun.). "Website of vestas wind power," [Online]. Available: http://www.vestas.com/

[25] Wind Turbines Overview. (2013, Jun.). "Website of vestas wind power," [Online]. Available: http://www.vestas.com/

[26] "User manual of PLECS blockset version 3.1," Mar. 2011.

[27] D. Graovac and M. Purschel, "IGBT power losses calculation using the data-sheet parameters," Infineon Technologies AG, Neubiberg, Germany, Jan. 2009.

[28] "Thermal equivalent circuit models," Infineon Application Note AN2008-03, Jun. 2008.

[29] "*Standard Practices Cycle Counting Fatigue Analysis*," ASTM International, IEEE Standard E1049-85, 2005.

[30] A. Niesłony, "Determination of fragments of multiaxial service loading strongly influencing the fatigue of machine components," *Mech. Syst. Signal Process.*, vol. 23, no. 8, pp. 2712–2721, 2009.

[31] P. Sørensen, A. D. Hansen, and P. A. C. Rosas, "Wind models for simulation of power fluctuations from wind farms," *J. Wind Eng.*, vol. 90, pp. 1381–1402, 2002.

[32] K. Ma, F. Blaabjerg, and M. Liserre, "Electro-thermal model of power semiconductors dedicated for both case and junction temperature estimation," in *Proc. PCIM*, 2013, pp. 1042–1046.

[33] K. Ma and F. Blaabjerg, "Multilevel converters for 10 MW wind turbines," in *Proc. 14th Eur. Conf. Power Electron. Appl.*, Aug. 2011, pp. 1–8.

[34] K. Ma and F. Blaabjerg, "Reliability-cost models for the power switching devices of wind power converters," in *Proc. IEEE 3rd Int. Symp. Power Electron. Distrib. Gen.*, 2012, pp. 820–827.

[35] N. kaminsku, "Load-cycling capability of HiPak," ABB Switzerland Ltd Semiconductors, Lenzburg, ABB Application Note 5SYA 2043-01, 2004.

[36] H. Wang, M. Liserre, F. Blaabjerg, P. de Place Rimmen, J. B. Jacobsen, T. Kvisgaard, and J. Landkildehus, "Transitioning to physics-of-failure as a reliability driver in power electronics," *IEEE J. Emerg. Sel. Topics Power Electron.*, vol. 2, no. 1, pp. 97–114, Mar. 2014.

[37] S. V. Dhople, A. Davoudi, A. D. Dominguez-Garci, and P. L. Chapman, "A unified approach to reliability assessment of multiphase DC–DC converters in photovoltaic energy conversion systems," *IEEE Trans. Power Electron.*, vol. 27, no. 2, pp. 739–751, Feb. 2012.

[38] R. Burgos, C. Gang, F. Wang, D. Boroyevich, W. G. Odendaal, and J. D. V. , "Reliability-oriented design of three-phase power converters for aircraft applications," *IEEE Trans. Aerosp. Electron. Syst.*, vol. 48, no. 2, pp. 1249–1263, Apr. 2012.

[39] K. Ma and F. Blaabjerg, "Lifetime estimation for the power semiconductors considering mission profiles in wind power converter," in *Proc. IEEE Energy Convers. Congr. Expo.*, Sep. 2013, pp. 2962–2971.

[40] D. Weiss and H. Eckel, "Fundamental frequency and mission profile wearout of IGBT in DFIG converters for wind power," in *Proc. 15th Eur. Conf. Power Electron. Appl.*, Sep. 2013, pp. 2–6.

[41] F. Fuchs and A. Mertens, "Steady state lifetime estimation of the power semiconductors in the rotor side converter of a 2 MW DFIG wind turbine via power cycling capability analysis," in *Proc. 14th Eur. Conf. Power Electron. Appl.*, Sep. 2011, pp. 1–8.

[42] K. Fischer, T. Stalin, H. Ramberg, T. Thiringer, J. Wenske, and R. Karlsson. (2012, Nov.). "Investigation of converter failure in wind turbines," Elforsk AB, Stockholm, Elforsk Report, [Online]. Avaiable: http://www.elforsk.se/

[43] M. Wilkinson, "Measuring wind turbine reliability, results of the reliawind project," Presented at the Eur. Wind Energy Conf. Exhib., Brussels, Belgium, 2011.

[44] F. Spinato, P. J. Tavner, G. J. W. van Bussel, and E. Koutoulakos, "Reliability of wind turbine subassemblies," *IET Renewable Power Gen.*, vol. 3, no. 4, pp. 387–401, 2009.
[45] K. Xie, Z. Jiang, and W. Li, "Effect of wind speed on wind turbine power converter reliability," *IEEE Trans. Energy Convers.*, vol. 27, no. 1, pp. 96–104, Mar. 2012.

Ke Ma (S'09–M'11) received the B.Sc. and M.Sc. degrees in electrical engineering from the Zhejiang University, Hangzhou, China, in 2007 and 2010, respectively, and the Ph.D. degree from the Aalborg University, Denmark, in 2013.

He is currently with the Department of Energy Technology, Aalborg University, Denmark, as a Postdoctoral Researcher. His research interests include the power electronics and reliability in the application of renewable energy generations.

Dr. Ma received the IEEE Industry Applications Society Industrial Power Converter Committee Third Prize Paper Award in 2012 and a prize paper award at ISIE Poland in 2011.

Marco Liserre (S'00–M'02–SM'O7–F'01) received the M.Sc. and Ph.D. degrees in electrical engineering from the Bari Polytechnic, Italy, in 1998 and 2002, respectively.

He has been an Associate Professor at Bari Polytechnic and a Professor in reliable power electronics at Aalborg University, Denmark. He is currently a Full Professor and a Chair of Power Electronics at Christian-Albrechts-University of Kiel, Germany. He has published 168 technical papers (44 of them in international peer-reviewed journals), three chapters of a book and a book (*Grid Converters for Photovoltaic and Wind Power Systems*, Wiley, also translated in Chinese). These works have received more than 6000 citations. He has been a Visiting Professor at Alcala de Henares University, Spain.

Dr. Liserre has been recently awarded with an ERC Consolidator Grant for an overall budget of 2 MEuro for the project "The Highly Efficient And Reliable smart Transformer (HEART), a new Heart for the Electric Distribution System." He is a member of the IAS, the PELS, the PES, and the IES. He is an Associate Editor of the IEEE TRANSACTIONS ON INDUSTRIAL ELECTRONICS, the IEEE INDUSTRIAL ELECTRONICS MAGAZINE, the IEEE TRANSACTIONS ON INDUSTRIAL INFORMATICS, where he is currently Co-EIC, IEEE TRANSACTIONS ON POWER ELECTRONICS and IEEE JOURNAL OF EMERGING AND SELECTED TOPICS IN POWER ELECTRONICS. He has been a Founder and an Editor-in-Chief of the IEEE INDUSTRIAL ELECTRONICS MAGAZINE, a Founder and the Chairman of the Technical Committee on Renewable Energy Systems, Cochairman of the International Symposium on Industrial Electronics (ISIE 2010), IES Vice-President responsible of the publications. He has received the IES 2009 Early Career Award, the IES 2011 Anthony J. Hornfeck Service Award, the 2011 Industrial Electronics Magazine best paper award and the Third Prize paper award by the Industrial Power Converter Committee at ECCE 2012, 2012. He is senior member of IES AdCom. In 2013, he has been elevated to the IEEE fellow grade with the following citation "for contributions to grid connection of renewable energy systems and industrial drives."

Frede Blaabjerg (S'86–M'88–SM'97–F'03) received the Ph.D. degree from Aalborg University, Denmark, in 1992.

He was with ABB-Scandia, Randers, Denmark, from 1987 to 1988. He became an Assistant Professor in 1992, an Associate Professor in 1996, and a Full Professor of power electronics and drives in 1998. His current research interests include power electronics and its applications such as in wind turbines, PV systems, reliability, harmonics and adjustable speed drives.

Dr. Blaabjerg has received 15 IEEE Prize Paper Awards, the IEEE PELS Distinguished Service Award in 2009, the EPE-PEMC Council Award in 2010, and the IEEE William E. Newell Power Electronics Award 2014. He was an Editor-in-Chief of the IEEE TRANSACTIONS ON POWER ELECTRONICS from 2006 to 2012. He has been a Distinguished Lecturer for the IEEE Power Electronics Society from 2005 to 2007 and for the IEEE Industry Applications Society from 2010 to 2011.

Tamás Kerekes (S'06–M'09) was born in 1978 in Cluj-Napoca, Romania. He received the Electrical Engineer diploma from Technical University of Cluj, Romania, with specialization in Electric Drives and Robots, in 2002, and the M.Sc. degree in the field of power electronics and drives and the Ph.D. degree in analysis and modeling of transformerless PV inverter systems both from the Institute of Energy Technology, Aalborg University, Denmark, in 2005 and September 2009, respectively.

He is currently employed as an Associate Professor and is doing research at the same institute within the field of grid-connected renewable applications. His research interest include grid-connected applications based on dc–dc, dc–ac single- and three-phase converter topologies focusing also on switching and conduction loss modeling and minimization in case of Si and new wide-bandgap devices.